Tetrahedron 68 (2012) 1230–1240

Contents lists available at SciVerse ScienceDirect

Tetrahedron

journal homepage: www.elsevier.com/locate/tet

Synthesis of SERS active nanoparticles for detection of biomolecules

Joanna Wrzesien, Duncan Graham *

Centre for Molecular Nanometrology, WestCHEM, Department of Pure and Applied Chemistry, University of Strathclyde, 295 Cathedral Street, Glasgow G1 1XL, UK

ARTICLE INFO

Article history:
Received 3 August 2011
Received in revised form 30 October 2011
Accepted 21 November 2011
Available online 29 November 2011

Keywords:
SERS
Nanoparticle
Linker
DNA

ABSTRACT

Surface Enhanced Raman Scattering (SERS) can be used to detect specific DNA sequences by methods based on hybridisation of oligonucleotide functionalized nanoparticles to complementary DNA sequences. The problem, which has to be overcome to use this technique is that DNA is not strongly SERS active. This is due to the lack of a visible chromophore and presence of the highly negatively charged phosphate backbone, which prevents the electrostatic interaction with the metal surface necessary for the enhancement. To obtain SERS active DNA a label containing a surface seeking group, to allow adsorption of DNA on a metal surface, and a chromophore has to be attached to the DNA strand. Here we report the synthesis of three linkers containing a Raman tag [the following fluorophores were used for this purpose due to the fluorescence quenching ability of metallic nanoparticles: fluorescein, 6-aminofluorescein and tetramethylrhodamine (TAMRA)], surface complexing group (cyclic disulphide—thioctic acid) and a chemical functionality for attachment of DNA (carboxyl group). Each of the linkers also contain poly(-ethylene glycol) (PEG) (3 *mer*), which reduces non-specific adsorption of molecules to the surface of the nanoparticles and provides colloidal stability. The synthesized linkers were used to functionalize gold citrate (18 and 50 nm), silver citrate (40 nm) and silver EDTA (35 nm) nanoparticles. All of the conjugates exhibit high stability, gave good SERS responses at laser excitation frequencies of 514 and 633 nm and could be conjugated to amino-modified oligonucleotides in the presence of the commonly used (*N*-(3-dimethylaminopropyl)-*N*′-ethyl carbodiimide hydrochloride—EDC·HCl with *N*-hydroxysulfosuccinimide or 4-(4,6-dimethoxy-1,3,5-triazin-2-yl)-4-methylmorpholinium chloride—DMT MM, which has not been used for bioconjugate preparation previously. This approach is less time consuming and less expensive than previously used protocols and does not require the formation of a mixed layer of oligonucleotides and Raman reporter on the metal surface. Additionally the presence of a reactive functionality within the linker structure makes it possible to conjugate the linker to other biomolecules of interest such as proteins.

1. Introduction

Development of simple, sequence specific DNA detection methods is one of the important areas of life science research. The majority of DNA detection methods require amplification of the target material by the polymerase chain reaction (PCR). The amplified product is then usually detected by fluorescence. These methods suffer from the need for amplification of the number of DNA copies present in the original sample and also the fluorescence spectra produced by these methods tend to have broad overlapping outputs thus limiting the multiplexing capacity of the technique. Alternatives to these traditional assays are methods based on hybridisation of silver or gold nanoparticles functionalized with oligonucleotides to the complementary target. These probes have numerous advantages, including rapid detection, colorimetric response, good selectivity and little or no instrumentation.[1–5] The hybridisation process can be monitored by UV–vis spectroscopy and also by Surface Enhanced Raman Scattering (SERS).[6–8] In this method surface enhancement provided by adsorption of the sample on a suitable metal surface and molecular resonance from the chromophore present in the analyte gives a vibrational spectrum with very high sensitivity.[6–10] The fingerprint spectra obtained by this technique make it possible to identify the components of a mixture without extensive separation procedures.[10,11] Since DNA does not meet the requirements for SERS due to the lack of a visible chromophore in the structure and also the presence of the highly negatively charged phosphate backbone, which prevents electrostatic interaction with the metal nanoparticles surface, a label containing a surface seeking group and a chromophore has to be attached to the DNA strand.[6,7,10,12]

To generate SERS active DNA a wide range of dyes and fluorescent labels (the metal surface used for enhancement quenches any

* Corresponding author. Tel.: +44 (0)141 548 4701; e-mail address: duncan.graham@strath.ac.uk (D. Graham).

0040-4020/$ – see front matter © 2011 Elsevier Ltd. All rights reserved.
doi:10.1016/j.tet.2011.11.053

fluorescence) can be used.[6,7,10,11] Fluoresceins and rhodamines are among the most commonly used fluorescent markers.[13,14] Fluoresceins exhibit high chemical and physical stability, are commercially available and are not expensive.[15–21] The main disadvantages of these dyes are relatively high photobleaching, pH sensitive fluorescence and a broad fluorescence emission spectrum.[14] The biggest advantages of rhodamines are their great photostability and pH insensitivity from low to neutral pH.[13]

Surface seeking groups are usually specific chemical functionalities, which can bind strongly to the metal nanoparticles and replace the weakly binding layer of charged ligands, which stabilize colloidal nanoparticles. In the case of gold nanoparticles, alkylthiols are commonly used for this purpose.[1,2,22,23] If the nanoparticles are to be functionalized with oligonucleotides then an alkylthiol modifier is usually added to one end of the oligonucleotides to allow the modified oligonucleotide to be attached to the gold nanoparticle surface. Dougan et al.[5] found that thioctic acid, a simple disulfide species, offered a greater stability of the conjugates, when used as a linker molecule, compared to thiol modified oligonucleotide nanoparticle conjugates. Further developments indicated that when a trithiol was used in the place of a cyclic disulfide, further increases in the stability of oligonucleotide functionalized nanoparticles was observed.[24,25] The hybridisation properties of the oligonucleotide functionalized nanoparticle conjugates prepared with monothiol, cyclic disulfide or trithiol modified oligonucleotides are comparable.[24,25]

In order to use the stability of the cyclic disulfide with nanoparticles in a SERS capacity, a specific resonant chromophore needs to be incorporated within the linker. This has to be done in such a way to ensure that the label is close enough to the surface to experience enhancement and the linker can still attach specific oligonucleotide probes to the nanoparticles. This would produce a nanoparticle with a permanent SERS signal and DNA hybridisation capabilities. Previously, thiolated oligonucleotides were used to functionalize gold and silver nanoparticles, which were then used in a hybridisation based assay.[2,3,26–29] Due to the lack of a visible chromophore in these conjugates the hybridisation of these probes to a complementary target could be monitored only by UV–vis spectroscopy.

To obtain SERS active oligonucleotide functionalized silver nanoparticles Thompson et al. pre-functionalized silver nanoparticles with a SERS active dye, then added thiolated DNA to formed SERS active oligonucleotide functionalized nanoparticles. The hybridisation of these probes to a complementary target was monitored by SERS.[9] The degree of enhancement of Raman scattering from nanoparticles can be significantly increased by aggregation of the nanoparticles, which was achieved by hybridisation in this case. Thus hybridisation effectively turned on the SERS, which was used to indicate hybridisation had occurred. McKenzie et al. described the use of linkers containing thioctic acid and a Raman active dye to pre-functionalize gold and silver nanoparticles. These linkers contained an additional reactive group (COOH), which enabled attachment of the biomolecules, in this case streptadivin.[30] In our approach linkers containing a cyclic disulfide, resonant chromophore and free carboxyl group were used to pre-functionalize metallic nanoparticles. The nanoparticle–linker conjugates can be reacted with amino-modified DNA to form nanoparticles with a permanent SERS signal and DNA hybridisation capabilities—which would change the SERS following hybridisation. This new type of linker offers improved ease of synthesis of dye tagged nanoparticles and simplifies the often-lengthy procedures commonly used.

2. Results and discussion

Fluorescent dyes are the most commonly used dyes in qualitative and quantitative chemical and biological analysis. Due to different combinations of properties (absorption and emission maxima, functional groups, polarity, microenvironmental-dependence of the fluorescence), which suits different applications, a large number of these dyes are used in bioscience research.[16] The largest advantages of these dyes are their high chemical and physical stability, commercial availability and low cost.[16–20,31] Rhodamines exhibit high molecular absorptivities in the visible region of the electromagnetic spectrum, great photostability and pH insensitivity over a broad range (low to neutral) and are commonly used as fluorescent markers. The absorption properties of these molecules are strongly dependant on the substituents present in the molecule.[13,14] In this work, synthesis of linkers containing one of the following chromophores—fluorescein, 6-aminofluorescein, tetramethylrhodamine (TAMRA); a surface seeking group—thioctic acid and a conjugation site (carboxyl group), to react with an amino-modified oligonucleotide and also 3 PEG units were designed. These linkers, when immobilised on metal surfaces enhance the stability of nanoparticles and also gives the opportunity to obtain a SERS response from a specific DNA sequence, which is itself not SERS active.

2.1. Synthesis of the 6-aminofluorescein linker

In order to synthesize the linker containing surface complexing group, Raman reporter, polyethylene glycol and free functionality, multifunctional molecules, such as lysine can be used as a core.[30] The use of such a molecule during synthesis of the 6-aminofluorescein linker was not necessary as 6-aminofluorescein itself contains two functional groups—aromatic amine, which could be reacted with the thioctic acid, and a phenol group, which after simple modification can be reacted with polyethylene glycol (Scheme 1). It is well known that fluoresceins can exist in a fluorescent, quinoid form, and a non-fluorescent lactoid form. The equilibrium between these two forms is reflected in the pH dependence of the fluorescence from fluoresceins. To overcome the tautomerization problem the fluorophore can be locked into its quinoid form by conjugation of its 2′ carboxylic group with a nucleophile (secondary amine[16,21] or alcohol[16,20,21,31]). It has been reported that the esterification of the 2′ carboxyl group of fluorescein gives an excellent yield[20,32] this method was chosen to lock 6-aminofluorescein into its quinoid form. In the first step of synthesis of an aminofluorescein linker, esterification of 6-aminofluorescein in refluxing acidic ethanol afforded ester **1**. The aim of the next step of this synthesis was to introduce a carboxyl functionality. Many ways to achieve this exist, such as alkylation of the 3′ phenol group using *tert*-butyl bromoacetate in the presence of *N*,*N*′-diisopropylethylamine (DIPEA) or potassium carbonate,[21,31] coupling of 3′*O*-(hydroxyalkyl) fluorescein methyl esters with dimethoxytrityl protected hydroxyalkyl chlorides under basic conditions[31] or alkylation of 3′ phenol group of fluoresceins methyl esters under Mitsunobu conditions.[31] Due to the previous work of Burchak et al.[20] indicating that alkylation of the 3′ phenol group do not involve the amine group and gives an excellent yield this method was used during synthesis of the aminofluorescein linker. Alkylation of **1** with *tert*-butyl bromoacetate in the presence of potassium carbonate in DMF followed by the cleavage of the *tert*-butyl ester using TFA in DCM afforded compound **3**. The free carboxyl group of the new moiety was then coupled with *tert*-butyl-12-amino-4,7,10-trioxadodecanoate in the presence of *O*-(7-azabenzotriazol-1-yl)-*N*,*N*,*N*′,*N*′-tetramethyluronium (HATU) and DIPEA to form **4**, which was then acylated with thioctic acid in the presence of *N*,*N*′-diisopropylcarbodiimide (DIC) to form, after cleavage of the *tert*-butyl ester group, the desired aminofluorescein linker **6** in 7% overall yield.

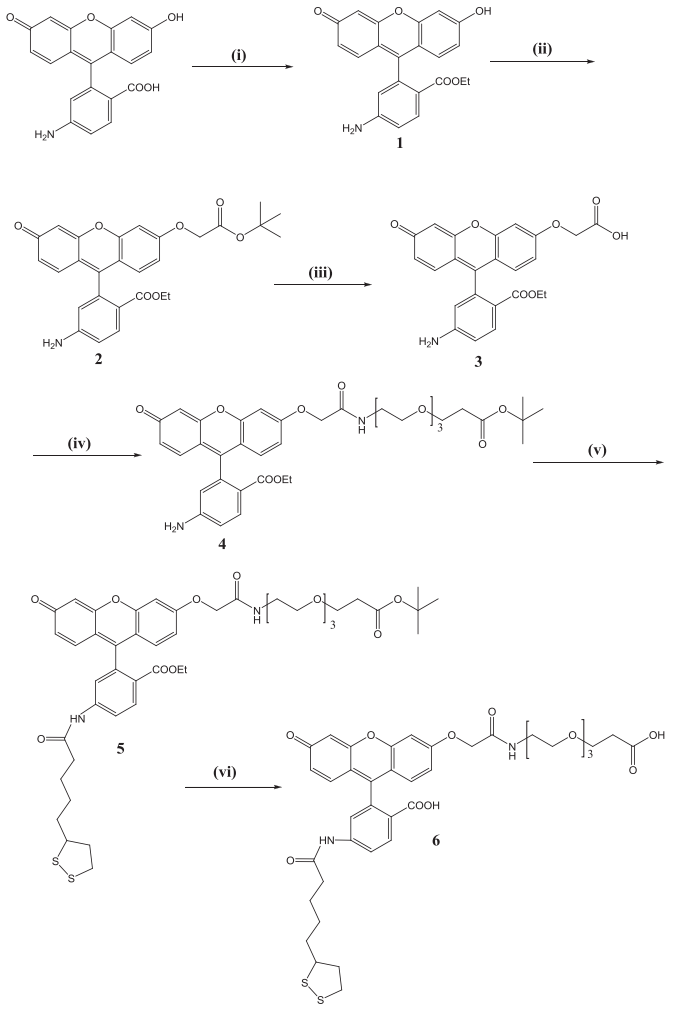

Scheme 1. Synthesis of the 6-aminofluorescein linker (**6**): (i) EtOH, H_2SO_4, 99%; (ii) $BrCH_2COOt$-Bu, K_2CO_3, DMF, 56%; (iii) TFA, DCM, 52%; (iv) *tert*-butyl-12-amino-4,7,10-trioxadodecanoate, HATU, DIPEA, DMF, 25%; (v) thioctic acid, DIC, DCM, 97%; (vi) TFA, DCM, 98%.

2.2. Synthesis of the fluorescein linker

A fluorescein linker was synthesized around a lysine core by the use of well known peptide coupling chemistry. To lock fluorescein into its fluorescent, quinoid form the 2′-carboxyl group of fluorescein was reacted with refluxing acidic ethanol to form ester **7**. Alkylation of the 3′ phenol group of the formed ester with *tert*-butyl bromoacetate in the presence of potassium carbonate followed by cleavage of the *tert*-butyl ester group by TFA afforded fluorescein derivative **9** (Scheme 2).

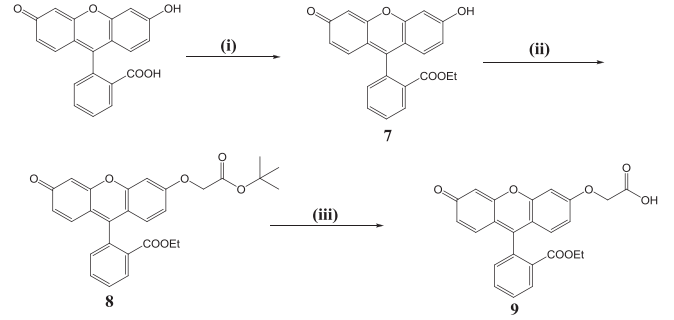

Scheme 2. Synthesis of 2-{9-[2-(ethoxycarbonyl)phenyl]-3-oxo-3*H*-xanthen-6-yloxy} acetic acid (**9**): (i) EtOH, H_2SO_4, 75%; (ii) $BrCH_2COOt$-Bu, K_2CO_3, DMF, 62%; (iii) TFA, DCM, 57%.

In the next step of the synthesis Fmoc–Lys(Boc)–OH was reacted with *tert*-butyl-12-amino-4,7,10-trioxadodecanoate in the presence of DIC to form molecule **10**. Chemoselective deprotection of the *N*-Boc group is a very important transformation in chemical synthesis. There are a large number of available reagents, which allow this transformation, such as strong acids (TFA, HCl, HBr, H_2SO_4, HNO_3, CF_3COOH) or Lewis acids ($ZnBr_3$, $BF_3 \cdot Et_2O$).[32,33] The deprotection can also be achieved under thermal[32] or neutral conditions (In, Zn).[33] The biggest disadvantage of the above procedures is lack of selectivity—these methods will remove both *N*-Boc and *tert*-butyl ester groups from the protected molecules. The other disadvantages of these methods are high acidity, strong oxidizing conditions, long reaction times and low yields.[32,33] The selectivity problems can be overcome by the use of bismuth(III) chloride in the mixture of acetonitrile and water (50:1, v/v) at 55 °C.[33] Under these conditions $BiCl_3$ selectively removes the *N*-Boc groups in the presence of *tert*-butyl esters. In the next step of the synthesis of the fluorescein linker the *N*-Boc group was selectively cleaved from molecule **10** in the presence of $BiCl_3$. The primary amine group was then reacted with thioctic acid in the presence of DIC to form molecule **12**. The Fmoc group was then removed from molecule **12** by use of a 20% solution of piperidine in acetonitrile (Scheme 3).

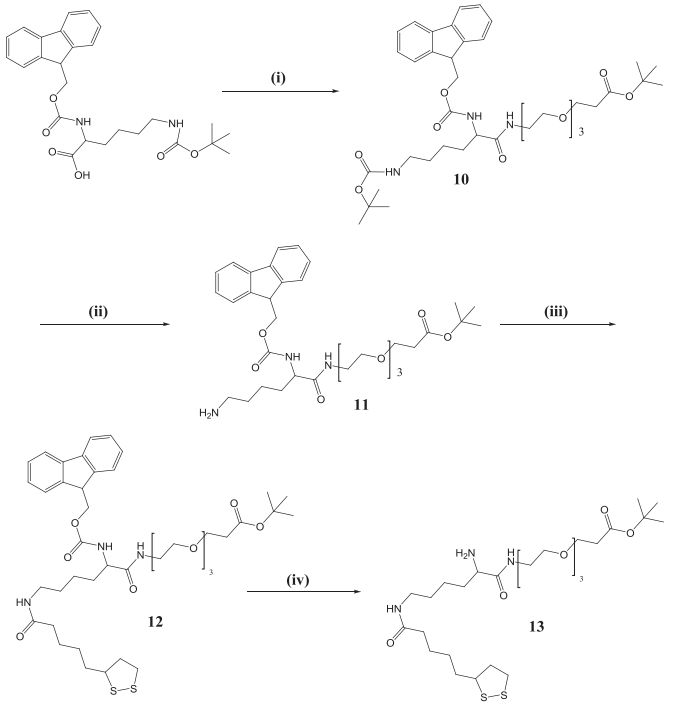

Scheme 3. Synthesis of the *tert*-butyl 15-amino-25-(1,2-dithiolan-3-yl)-14,21-dioxo-4,7,10-trioxa-13,20-diazapentacosan-1-oate (**13**): (i) *tert*-butyl-12-amino-4,7,10-trioxadodecanoate, DIC, DCM, 92%; (ii) $BiCl_3$, CH_3CN/H_2O, 31%; (iii) thioctic acid, DIC, DCM, 29%; (iv) 20% piperidine, CH_3CN, 92%.

Coupling of the fluorescein derivative **9** with *tert*-butyl 15-amino-25-(1,2-dithiolan-3-yl)-14,21-dioxo-4,7,10-trioxa-13,20-diazapentacosan-1-oate (**13**) in the presence of HATU and DIPEA followed by cleavage of *tert*-butyl ester afforded fluorescein linker **15** with an overall yield of 3% (Scheme 4).

2.3. Synthesis of the TAMRA linker

Similarly to the fluorescein linker a TAMRA linker was synthesized around a lysine core. In the first step of the synthesis of the TAMRA linker Fmoc–Lys(Boc)–OH was coupled with *tert*-butyl-12-amino-4,7,10-trioxadodecanoate in the presence of DIC to produce the amide **10** (Scheme 3). After cleavage of the Fmoc group in the

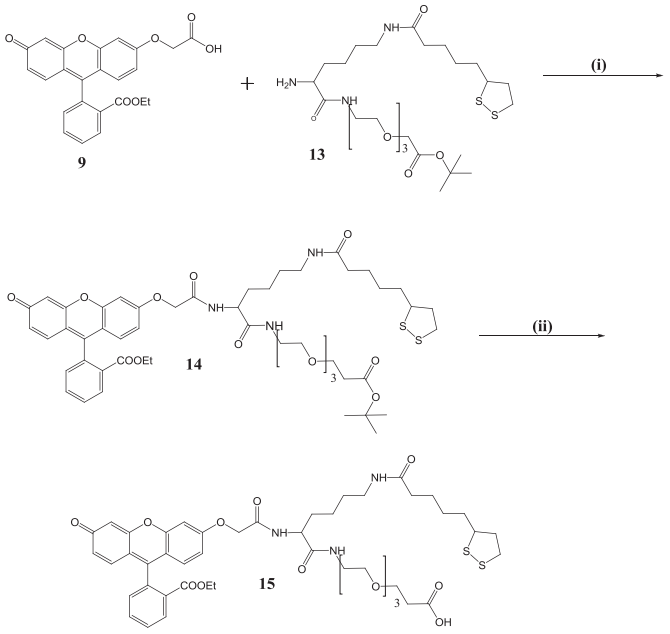

Scheme 4. Synthesis of the fluorescein linker (**15**): (i) HATU, DIPEA, DMF, 60%; (ii) TFA, DCM, 57%.

presence of piperidine in acetonitrile, **16** was coupled with thioctic acid in the presence of DIC. Both the *N*-Boc and *tert*-butyl groups were removed from **17** using TFA in DCM (1:1) giving **18**. In contrast to fluorescein, which exists in a non-fluorescent lactoid form at acidic pH, rhodamines can exist in a fluorescent quinoid form at neutral and acidic pH. The non-fluorescent lactoid form only exists at basic pH.[13] A large number of rhodamine conjugates are synthesized from 4′ or 5′ activated rhodamine derivatives (active ester, acid chloride).[1] In the synthesis of this TAMRA linker the succinimidyl ester of 5-tetramethyl rhodamine (TAMRA SE) was used. This molecule was coupled with **18** to give the desired TAMRA linker (**19**) in 27% overall yield (Scheme 5).

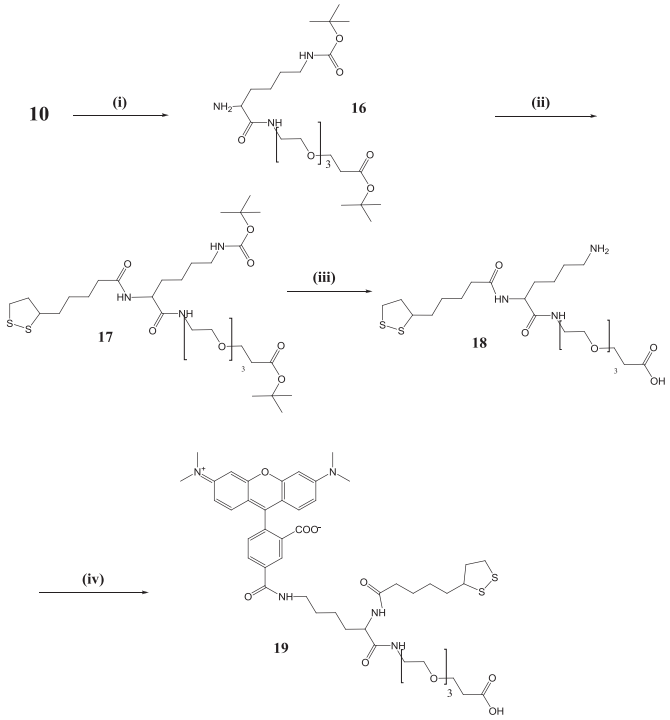

Scheme 5. Synthesis of the TAMRA linker (**19**): (i) 20% piperidine, CH_3CN, 92%; (ii) thioctic acid, DIC, DCM, 85%; (iii) TFA, DCM, 89%; (iv) TAMRA SE, 37%.

2.4. SERS active nanoparticle–linker conjugates

All of the synthesized linkers were used to functionalize the following types of nanoparticles: citrate stabilized Au (18, 50 nm), citrate stabilized Ag (40 nm), EDTA stabilized Ag (40 nm).

The plasmon band of the nanoparticles was red shifted after addition of the linkers (typically 2–4 nm), which confirmed the modification of the nanoparticle surface. Covalent attachment of the linkers to the surface of the nanoparticles was also confirmed by gel electrophoresis (Fig. 1). The attachment of the aminofluorescein linker to the Au nanoparticles caused an increase in the mobility of the nanoparticles in agarose gel. The opposite was observed for Ag EDTA nanoparticles functionalized with the same linker. The same was observed for all types of conjugates prepared. It has been reported[34] that only covalent attachment of a molecule to a nanoparticle surface causes changes in the nanoparticle mobility in agarose gel. This means that the mobility of bare nanoparticles is the same as the mobility of nanoparticles with oligonucleotides electrostatically attached to their surface, i.e., they don't move.

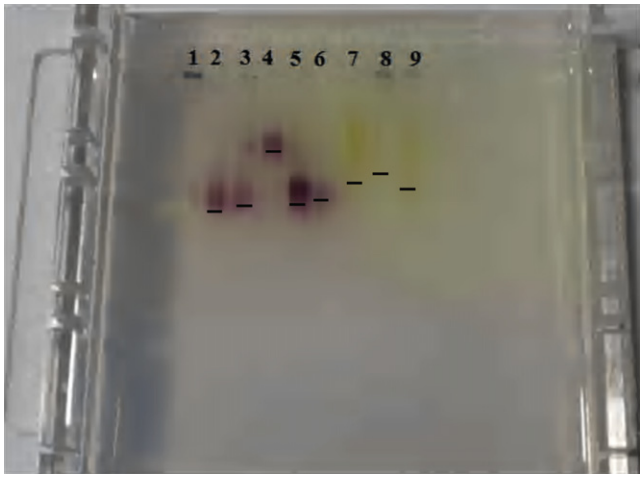

Fig. 1. Agarose gel (1.5%, 0.5×TBE, 60 min, 120 mV) of all the aminofluorescein conjugates: 1—18 nm Au colloid; 2—18 nm Au–**6**; 3—18 nm Au–**6**–DNA; 4—50 nm Au colloid; 5—50 nm Au–**6**; 6—50 nm Au–**6**–DNA; 7—AgEDTA colloid; 8—AgEDTA–**6**; 9—AgEDTA–6–DNA.

The number of linker molecules attached to each type of nanoparticles was calculated using the method described by Demers et al.[23] (Table 1). The only exception was the 50 nm Au nanoparticles functionalized with the 6-aminofluorescein linker. Dithiothreitol did not displace the linker from the nanoparticle surface hence the lack of value for this conjugate. The highest surface coverage was obtained for nanoparticles functionalized with the TAMRA linker.

Zeta particle size and zeta potential of all linker–nanoparticle conjugates were measured (Tables 2 and 3). As expected the hydrodynamic diameter of both types of Au nanoparticles slightly increased after attachment of a linker. Interestingly the size of linker modified silver nanoparticles (citrate and EDTA stabilized) was smaller than the size of the bare silver nanoparticles. This is likely due to the fact that the electrostatic and steric repulsion potential of the modified nanoparticles is higher than the one for bare nanoparticles. Therefore the repulsive force between linker–nanoparticle conjugates is larger than the same force between citrate or EDTA capped nanoparticles. Linker functionalized silver nanoparticles are better separated from each

Table 1
Number of linker molecules and oligonucleotides attached to the nanoparticles examined

Linker	Type of nps	No of linker molecules attached to one np/surface coverage [pmol/cm^2]	Coupling agent	No of oligonucleotides attached to one np/surface coverage [pmol/cm^2][b]
Af	18 nm Au	298±29	EDC·HCl	0.31±0.01 0.097±0.004
		93±9	DMT MM	0.51±0.03 0.16±0.009
	50 nm Au	—	EDC·HCl	9.36±1.53 0.23±0.04
			DMT MM	11.33±3.75 0.28±0.09
	Ag citrate	4202±282	EDC·HCl	—
		139±21	DMT MM	—
	Ag EDTA	578±62	EDC·HCl	—
		15±4	DMT MM[a]	63.04±0.17 2.09±0.007
F	18 nm Au	90±33	EDC·HCl	0.16±0.036 0.026±0.006
		28±10	DMT MM	0.18±0.028 0.029±0.005
	50 nm Au	3248±220	EDC·HCl	—
		107±7	DMT MM	—
	Ag citrate	2145±388	EDC·HCl	—
		70±12	DMT MM	—
	Ag EDTA	1653±158	EDC·HCl	—
		54±5	DMT MM	144.42±11.55 4.78±0.38
T	18 nm Au	8100±324	EDC·HCl	9.48±0.29 1.54±0.05
		2547±102	DMT MM	9.23±0.53 1.50±0.08
	50 nm Au	26,927±787	EDC·HCl	—
		890±26	DMT MM	—
	Ag citrate	114,000±2080	EDC·HCl	—
		3780±69	DMT MM	—
	Ag EDTA	5613±940	EDC·HCl	—
		185±31	DMT MM[a]	1646±174 54.42±5.75

Af—aminofluorescein linker; F—fluorescein linker, T—TAMRA linker.
[a] Conjugation reaction was performed in water.
[b] If not otherwise stated the conjugation reaction was performed in 10 mM phosphate buffer pH=7.6.

Table 2
Zeta particle size of prepared conjugates

Linker	Type of nanoparticles	Zeta average size of colloid [nm]	Zeta average size of linker functionalized nanoparticles [nm]	Zeta average size of oligonucleotide–linker–nanoparticle conjugates [nm]
A	18 nm Au	46.70±0.94	50.90±0.70	55.7±0.90
	50 nm Au	51.63±0.25	54.13±1.25	56.40±0.26
	Ag citrate	87.00±1.87	78.40±1.97	—
	AgEDTA	58.46±1.00	55.93±1.56	94.65±8.98
F	18 nm Au	46.70±0.94	46.1±0.61	47.37±0.83
	50 nm Au	50.10±0.36	53.33±0.60	—
	Ag citrate	87.00±1.87	83.30±1.70	—
	AgEDTA	58.46±1.00	59.33±1.14	59.73±3.44
T	18 nm Au	53.43±0.55	52.93±1.95	57.17±5.08
	50 nm Au	50.10±0.36	70.40±1.83	—
	Ag citrate	87.00±1.87	77.80±2.02	—
	AgEDTA	58.46±1.00	56.40±0.20	67.67±0.81

The concentrations of the samples were as follows: 18 nm Au conjugates: 7.95×10^{-10} M, 50 nm Au conjugates 2.52×10^{-11} M, silver nanoparticles conjugates 3×10^{-11} M.

other than unmodified silver nanoparticles, thus the decrease of the hydrodynamic diameter is observed after surface modification.

High zeta potential values obtained for most of the linker–nanoparticle conjugates indicate that the modified nanoparticles exhibit high stability. For 18 nm Au nanoparticles functionalized with the TAMRA linker the zeta potential changes from −56.3 to −24.8 mV after surface modification, which is caused by the addition of the positively charged reporter moiety. The same behaviour was observed for other types of conjugates prepared with the TAMRA linker.

SERS spectra from all of the prepared conjugates were taken at three different laser excitation frequencies 514, 633 and 785 nm. As expected none of the conjugates gave a good SERS response with a laser excitation frequency of 785 nm. The excitation frequency was not close enough to the absorption maximum of the dyes (557 nm for TAMRA, 495 nm for 6-aminofluorescein, 495 nm for fluorescein) or the plasmon of the metal nanoparticles (400 nm for

Table 3
Zeta potential of prepared conjugates

Linker	Type of nanoparticles	Zeta potential of colloid [mV]	Zeta potential of linker functionalized nanoparticles [mV]	Zeta potential of oligonucleotide–linker–nanoparticle conjugates [mV]
A	18 nm Au	−37.7±9.0	−44.7±8.1	−46.0±8.5
	50 nm Au	−34.3±4.0	−47.9±2.9	−21.8±6.3
	Ag citrate	−33.4±3.6	−35.6±5.5	—
	AgEDTA	−37.0±4.7	−40.3±5.4	−13.2±5.1
F	18 nm Au	−34.5±9.0	−29.4±3.4	−32.1±1.7
	50 nm Au	−29.5±6.0	−26.7±2.2	—
	Ag citrate	−33.4±3.6	−35.1±3.8	—
	AgEDTA	−37.0±4.7	−42.4±3.0	−13.1±5.3
T	18 nm Au	−56.3±6.5	−24.8±5.6	−30.5±3.6
	50 nm Au	−34.3±4.0	−27.0±3.5	—
	Ag citrate	−33.4±3.6	−22.2±2.9	—
	AgEDTA	−37.0±4.7	−22.0±3.5	−8.7±3.3

The concentrations of the analyzed samples were as follows: 18 nm Au conjugates: 2.65×10^{-10} M, 50 nm Au conjugates: 8.4×10^{-12} M, silver nanoparticles conjugates 1×10^{-11} M.

Ag, 520 nm for Au). Nanoparticles functionalized with the TAMRA linker gave a better SERS response at 633 nm (Fig. 1). For 6-aminofluorescein conjugates good SERS spectra were obtained at 514 and 633 nm (Fig. 2). In the case of the fluorescein linker conjugates the weakest SERS signals were obtained when compared with TAMRA and aminofluorescein linker functionalized nanoparticles. Fluorescein and 6-aminofluorescein have very similar chemical structures. The difference in SERS response of the two linkers containing fluorescein derivatives is caused by the different geometry of synthesized linkers. In the case of the 6-aminofluorescein linker, the fluorescent label is closer to the metal surface after attachment of the linker to the nanoparticles and it experiences a larger enhancement to give a stronger SERS signal.

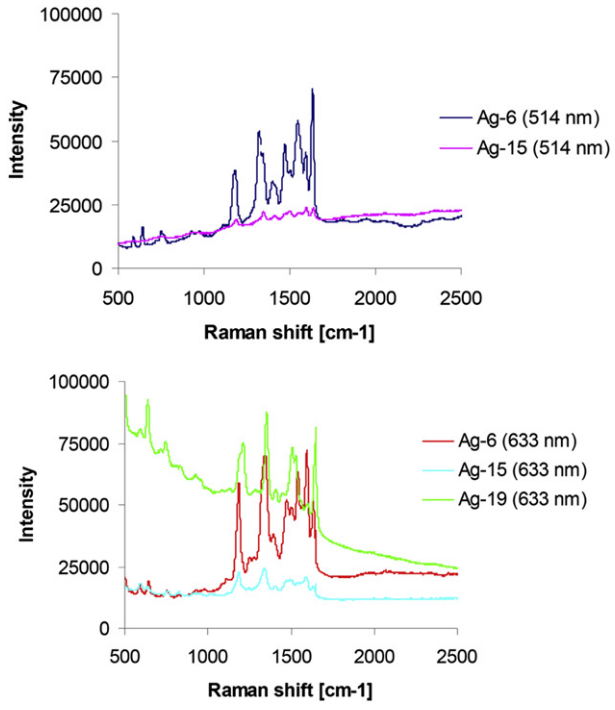

Fig. 2. SERS spectra of Ag citrate nanoparticles functionalized with different linkers (Af, F, T) at different laser excitation frequencies.

2.5. Oligonucleotide functionalized nanoparticles

Two different coupling chemistries were used to conjugate linker–nanoparticles to amino-modified oligonucleotides. One of them, commonly used for bioconjugate preparation used *N*-(3-dimethylaminopropyl)-*N*′-ethyl carbodiimide hydrochloride—EDC·HCl with *N*-hydroxysulfosuccinimide. The second, novel method adopts 4-(4,6-dimethoxy-1,3,5-triazin-2-yl)-4-methylmorpholinium chloride—DMT MM as an amide bond forming reagent in a simple one-step process. Both types of coupling reactions were performed in 10 mM phosphate buffer pH=7.6. When DMT MM was used as a coupling agent the conjugation reaction could also be performed in water.[35,36]

In the case of 18 nm Au nanoparticles functionalized with all types of synthesized linkers and 50 nm Au nanoparticles functionalized with aminofluorescein linker, both coupling chemistries were successfully used to conjugate functionalized nanoparticles to oligonucleotides. Both types of silver nanoparticles used were not stable after functionalisation with the linkers in 10 mM phosphate buffer, thus these conjugates could not be reacted with amino-modified oligonucleotides in the presence of EDC·HCl. The same was observed for 50 nm Au nanoparticles functionalized with the TAMRA and fluorescein linkers. In the case of Ag EDTA nanoparticles functionalized with all types of linkers the conjugation reaction could be performed when DMT MM in water was used, however probes formed in that process were not stable in buffers usually used for DNA hybridisation. Larger Au and Ag nanoparticles would probably require a longer PEG unit to be incorporated into the linker to form stable, SERS active probes.

Covalent attachment of oligonucleotides to linker–nanoparticle conjugates was confirmed by gel electrophoresis (Fig. 1). In the case of the 18 nm Au nanoparticles functionalized with the aminofluorescein linker prior and after conjugation to oligonucleotides (performed in water in the presence of DMT MM) a very small difference in nanoparticle mobility was observed. This is due to the fact that there is a very small amount of DNA attached to the nanoparticles. The same trend was observed for larger Au nanoparticles functionalized with the same linker. Addition of the aminofluorescein linker to Ag EDTA nanoparticles decreased the mobility of these nanoparticles, due to an increase in size of the conjugates, however attachment of the oligonucleotides (negative charge) caused it to increase. The changes in mobility of nanoparticles in the agarose gel are caused by the change in size and charge of the conjugates, due to covalent attachment to the surface of the nanoparticle.[34] Similar results were obtained for all of the conjugates.

The number of DNA strands attached to one nanoparticle for all prepared conjugates was calculated using the DNAse 1 method described by McKenzie et al.[37] (Table 1). Both coupling agents used exhibit similar effectiveness during functionalisation of Au nanoparticles with oligonucleotides in phosphate buffer. When DMT MM in water was used to conjugate 18 nm Au nanoparticles

functionalized with the TAMRA linker to oligonucleotides the coupling reaction was much more effective than the same process performed using both coupling chemistries in phosphate buffer. It was found that 22.76±9.65 DNA strands (3.71±1.57 pmol/cm^2) attached to 1 Au nanoparticle when the coupling reaction was performed in water, in the presence of DMT MM; only about 10 DNA strands attached to 1 nanoparticle when the coupling reaction was performed in phosphate buffer in the presence of both types of amide bond forming agents. Observed lower yield of the conjugation reaction performed in the phosphate buffer might be caused by the screening effect of the salt ions present in the reaction mixture. DMT MM was found to be a less costly, more efficient amide bond forming reagent allowing the preparation of bioconjugates in a simple, one-step process performed in water. The novel method presented here offers improved ease of dye tagged nanoparticles and simplifies the often-lengthy procedures commonly used.

Zeta particle size and zeta potential of all nanoparticle–linker–DNA conjugates were measured (Tables 2 and 3). For most of the conjugates a small increase in the hydrodynamic diameter was observed after DNA attachment. For Ag EDTA–**6**–DNA a large increase in the hydrodynamic size was observed after conjugation of oligonucleotides. The results indicate that small aggregates (dimers, trimers) were formed during conjugation of Ag EDTA–**6** to oligonucleotides.

For all types of Au–linker–DNA conjugates the zeta potential was slightly higher (more negative) than for the nanoparticles prior to conjugation of oligonucleotides. This is caused by the addition of negatively charged DNA to the conjugates. In the case of all the Ag EDTA–linker conjugates, a large decrease in zeta potential after oligonucleotide attachment was observed. This indicates that the stability of oligonucleotide functionalized Ag EDTA nanoparticles is very low. The large increase in the intensity of the SERRS signal observed at 633 nm from Ag EDTA nanoparticles functionalized with the TAMRA linker after conjugation to oligonucleotides confirms that nanoparticle aggregates were formed during the conjugation process (Fig. 3).

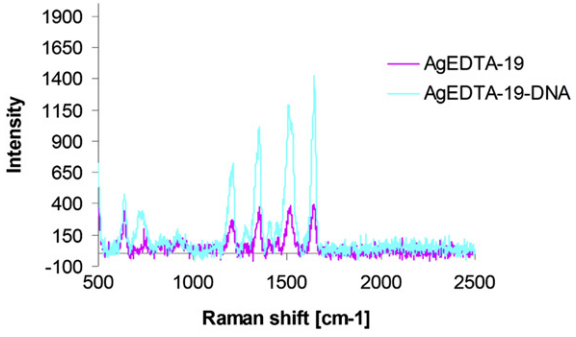

Fig. 3. SERRS spectra of the Ag EDTA–TAMRA linker (**19**) conjugates prior and after oligonucleotides attachment at 633 nm.

SERRS spectra of 18 nm Au nanoparticles functionalized with the TAMRA linker (19) prior and after oligonucleotide attachment are presented in Fig. 4. In this case a small increase in the intensity of the SERRS signal was observed after conjugation to oligonucleotides. We attribute this to small number of dimers and trimers formed, which have a dramatic affect on the signal.

3. Conclusions

The aim of the presented work was to develop a less time consuming method to allow preparation of SERS active

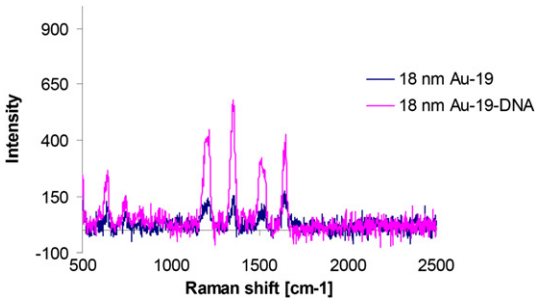

Fig. 4. SERRS spectra of the Au–TAMRA linker (**19**) conjugates prior and after oligonucleotides attachment at 633 nm.

nanoparticles, which could be conjugated to biomolecules such as DNA. This was achieved by functionalisation of the metal surface with multifunctional linkers containing a surface complexing group, Raman tag and functionality to allow biomolecule attachment. Three linkers, which can be used for that purpose were successfully synthesized. These linkers were used for preparation of conjugates with the following types of nanoparticles: 18 and 50 nm gold citrate, silver citrate and silver EDTA. TAMRA linker conjugates gave a good SERS response at the laser excitation frequency of 633 nm. In the case of fluorescein and aminofluorescein linkers, SERS signals were obtained at the laser excitation frequencies of 514 and 633 nm. The better SERS response was obtained for the aminofluorescein linker. Despite the very similar chemical structure of the fluorescent dyes used for the synthesis of those linkers, the geometry of the linkers is different. In the case of the aminofluorescein linker after adsorption on the nanoparticle surface, the label is closer to the metal surface and thus experiences a bigger enhancement.

Two different coupling agents were used to conjugate linker functionalized nanoparticles to oligonucleotides: *N*-(3-dimethylaminopropyl)-*N*′-ethyl carbodiimide hydrochloride—EDC·HCl with *N*-hydroxysulfosuccinimide or 4-(4,6-dimethoxy-1,3,5-triazin-2-yl)-4-methylmorpholinium chloride—DMT MM. The coupling reactions were performed in phosphate buffer or in water when DMT MM was used as an amide bond forming reagent. Due to the low stability of both types of silver nanoparticles and 50 nm Au nanoparticles, the functionalisation with oligonucleotides was not successful. In the case of Ag EDTA nanoparticles the preparation of oligonucleotide conjugates was possible when DMT MM in water was used as a coupling agent, however the formed conjugates were not stable in buffers usually used for DNA hybridisation. In the case of 18 nm gold nanoparticles functionalized with all types of linkers and 50 nm Au nanoparticles functionalized with the aminofluorescein linker, oligonucleotide functionalized probes could be prepared using both coupling chemistries. Both coupling reagents exhibit similar effectiveness when the coupling reaction was performed in phosphate buffer, however DMT MM was much more effective when the coupling reaction was performed in water. The prepared oligonucleotide functionalized nanoparticles were stable in buffers usually used for DNA hybridisation for several weeks. These synthesized linkers allow simple fabrication of SERS active metallic nanoparticles applicable not only for DNA based assemblies, but also to other biomolecules such as proteins due to the coupling chemistry reported.

4. Experimental

4.1. General methods

Reagents were purchased from Aldrich, Acros Organics, Alfa Aesar, Ana Spec or Cambridge Bioscience Ltd and used without further purification. ^{1}H NMR and ^{13}C NMR experiments were

recorded on a Bruker DPX 400 MHz spectrometer with the appropriate solvent peak as a reference. *J* values are quoted in hertz. Mass spectrometry was carried out as a service by the EPSRC National Mass Spectrometry Service Centre, Swansea.

4.2. Synthesis of the 6-aminofluorescein linker

*4.2.1. Ethyl 4-amino-2-(6-hydroxy-3-oxo-3H-xanthen-9-yl)benzoate (**1**) (ethyl 2-(6-hydroxy-3-oxo-3H-xanthen-9-yl)benzoate (**7**)).* H_2SO_4 (A: 0.77 ml, 14.4 mmol; B: 0.80 ml, 15.00 mmol) was added dropwise to the suspension of 6-aminofluorescein (A) (1.00 g, 2.88 mmol) or fluorescein (B) (1.000 g, 3.0 mmol) in EtOH. After stirring at reflux for 24 h the EtOH was removed under reduced pressure. The residue was diluted in $CHCl_3$ with a few drops of MeOH. Solid $NaHCO_3$ was added until gas evolution ceased. The resulting mixture was filtered, then the organic phase was dried over anhydrous Na_2SO_4, filtered and concentrated under reduced pressure. The residue was subjected to silica gel chromatography eluting with EtOAc, then MeOH/DCM (1:9) to afford the title compound as a dark orange solid (**1**) (1.082 g, 99%) or brown solid (**7**) (0.814 g, 75%).

Compound **1**: ^{1}H NMR (400 MHz, DMSO) δ 0.86 (3H, t, 7.1, CH_3), 3.71 (2H, q, 7.1, CH_2), 6.43 (1H, s, CH), 6.66 (4H, d, 7.4, 4×CH), 6.78 (1H, d, 8.7, CH), 7.01 (2H, d, 9.7, 2×CH), 7.89 (1H, d, 8.7, CH). ^{13}C NMR (100.62 MHz, DMSO) δ 13.50, 15.09, 59.62, 61.07, 102.92, 113.57, 113.97, 114.60, 115.15, 130.50, 132.81, 135.81, 152.83, 164.58. LRMS 376.20 [$(M+H)^+$] ($C_{22}H_{18}O_5N$ requires 376.62).

Compound **7**: ^{1}H NMR (400 MHz, DMSO) δ 0.83 (3H, t, 8.0, CH_3), 3.91 (2H, q, 8.0, CH_2), 5.75 (1H, s, OH), 7.07 (2H, d, 10.0, 2×CH), 7.22 (2H, s, 2×CH), 7.29 (2H, d, 12.0, 2×CH), 7.54 (1H, d, 6.0, CH), 7.86 (1H, t, 8.0, CH), 7.93 (1H, t, 8.0, CH), 8.28 (1H, d, 8.0, CH). ^{13}C NMR (100.62 MHz, DMSO) δ 13.29, 15.10, 61.11, 61.24, 102.35, 116.13, 120.56, 129.43, 130.15, 130.88, 130.97, 132.62, 133.18, 158.32, 164.50, 171.35. HRMS 361.11 [$(M+H)^+$] ($C_{22}H_{17}O_5$ requires 361.17).

*4.2.2. Ethyl 4-amino-2-[(6-tert-butoxy-2-oxoethoxy)-3-oxo-3H-xanthen-9-yl]benzoate (**2**) (ethyl 2-[6-(2-tert-butoxy-2-oxoethoxy)-3-oxo-3H-xanthen-9-yl]benzoate (**8**)).* *tert*-Butyl bromoacetate (**2**: 0.47 ml, 3.17 mmol; **8**: 0.37 ml, 2.48 mmol) was added to the mixture of compound **1** (1.082 g, 2.88 mmol) or **7** (0.814 g, 2.26 mmol) and K_2CO_3 (1:0.44 g, 3.17 mmol; 7: 0.34 g, 2.48 mmol) in the minimum amount of DMF. After stirring for 3 h at room temperature the reaction mixture was diluted with H_2O and extracted with EtOAc (3×20 ml). The organic phase was washed with 1 M $NaHCO_3$ and satd NaCl, then dried over anhydrous Na_2SO_4, filtered and concentrated under reduced pressure. The residue was subjected to silica gel chromatography eluting with EtOAc, then MeOH/DCM (1:9) giving 0.79 g (**2**) or 0.66 g (**8**) of title compound as orange solids (**2**: 56%; **8**: 62%).

Compound **2**: ^{1}H NMR (400 MHz, DMSO) δ 0.84(3H, t, 7.1, CH_3), 1.43 (9H, s, $C(CH_3)_3$), 3.81–3.89 (2H, m, CH_2), 4.86 (2H, s, CH_2), 6.21 (1H, s, CH), 6.39–6.45 (2H, m, 2×CH), 6.77 (1H, d, 7.6, CH), 6.90 (3H, m, 3×CH), 7.16 (1H, s, CH), 7.89 (1H, d, 8.7, CH). ^{13}C NMR (100.62 MHz, DMSO) δ 13.54, 27.68, 59.62, 81.80, 104.44, 113.42, 129.01. LRMS 490.76 [$(M+H)^+$] ($C_{28}H_{28}O_7N$ requires 490.20).

Compound **8**: ^{1}H NMR (400 MHz, DMSO) δ 0.85 (3H, t, 8.0, CH_3), 1.42 (9H, s, $C(CH_3)_3$), 3.92–4.05 (2H, m, CH_2), 4.87 (2H, s, CH_2), 6.44 (1H, s, CH), 6.38 (1H, d, 8.0, CH), 6.80–6.92 (3H, m, 3×CH), 7.20 (1H, s, CH), 7.50 (1H, d, 8.0, CH), 7.76 (1H, t, 4.0, CH), 7.79 (1H, t, 8.0, CH), 8.18 (1H, d, 8.0, CH). ^{13}C NMR (100.62 MHz, $CDCl_3$) δ 13.86, 13.92, 28.40, 53.73, 61.74, 104.14, 114.01, 115.33, 122.43, 129.60, 130.08, 130.60, 130.79, 130.91, 131.02, 131.52, 131.61, 132.76, 132.91, 134.38, 135.52, 155.47, 158.01, 165.70, 175.75. HRMS 475.1751 [$(M+H)^+$] ($C_{28}H_{27}O_7$ requires 475.1751).

*4.2.3. 2-{9-[5-Amino-2-(ethoxycarbonyl)phenyl]-3-oxo-3H-xanthen-6-yloxy}acetic acid (**3**) (2-{9-[2-(ethoxycarbonyl)phenyl]-3-oxo-3H-xanthen-6-yloxy}acetic acid (**9**)).* TFA (3 ml) was added to the solution of **2** (0.79 g, 1.61 mmol) or **8** (0.66 g, 1.40 mmol) in DCM (3 ml). After stirring for 3 h at room temperature DCM and TFA were evaporated. The residue was solidified by addition of diethyl ether, then it was filtered and washed with the same solvent giving after drying 0.36 g of the title compound as an orange solid (52%) (**3**) or 0.33 g of the title compound as a dark yellow solid (57%) (**9**).

Compound **3**: ^{1}H NMR (400 MHz, DMSO) δ 0.85 (3H, t, 5.7, CH_3), 3.82–3.89 (2H, m, CH_2), 4.96 (2H, s, CH_2), 6.46 (1H, s, CH), 6.55 (1H, s, CH), 6.64 (1H, d, 7.7, CH), 6.81 (1H, d, 7.0, CH), 7.05 (1H, d, 7.2, CH), 7.13–7.16 (2H, m, 2×CH), 7.33 (1H, s, CH), 7.91 (1H, d, 8.7, CH). ^{13}C NMR (100.62 MHz, DMSO) δ 13.54, 59.74, 65.23, 101.16, 103.78, 113.77, 113.97, 115.07, 115.34, 116.42, 131.44, 132.84, 135.55, 152.89, 154.51, 158.69, 164.54, 169.21. LRMS 434.20 [$(M+H)^+$] ($C_{24}H_{20}O_7N$ requires 434.70).

Compound **9**: ^{1}H NMR (400 MHz, DMSO) δ 0.86 (3H, t, 7.1, CH_3), 3.93–4.01 (2H, m, CH_2), 4.95 (2H, s, CH_2), 6.49 (1H, s, CH), 6.57 (1H, d, 9.6, CH), 6.95–7.04 (3H, m, 3×CH), 7.32 (1H, s, CH), 7.52 (1H, d, 7.6, CH), 7.79 (1H, t, 7.7, CH), 7.87 (1H, t, 7.5, CH), 8.21 (1H, d, 8.2, CH). ^{13}C NMR (100.62 MHz, DMSO) δ 13.32, 60.96, 65.16, 101.28, 104.22, 114.62, 129.42, 129.83, 130.19, 130.49, 130.71, 130.87, 169.26. HRMS 419.40 [$(M+H)^+$] ($C_{24}H_{19}O_7$ requires 419.20).

*4.2.4. tert-Butyl 1-{[9-(5-amino-2-ethoxycarbonyl)phenyl]-3-oxo-3H-xanthen-6-yloxy}-2-oxo-6,9,12-trioxa-3-azapentadecan-15-oate (**4**).* Compound **3** (0.36 g, 0.83 mmol) was dissolved in small amount of DMF. HATU (0.378 g, 0.995 mmol) and DIPEA (0.32 g, 2.500 mmol) were added. After stirring for 15 min at room temperature *tert*-butyl-12-amino-4,7,10-trioxadodecanoate (0.23 g, 0.83 mmol) was added. After stirring for 3 h at room temperature another portions of HATU (0.378 g, 0.995 mmol) and DIPEA (0.32 g, 2.50 mmol) were added. After stirring for another 20 h at room temperature the reaction mixture was diluted with water, then extracted with Et_2O (3×20 ml). The organic phase was dried over anhydrous Na_2SO_4, filtered and concentrated under reduced pressure. The residue was subjected to silica gel chromatography eluting with MeOH/DCM 1–20% giving 0.142 g of the title compound (25%) as an orange solid. ^{1}H NMR (400 MHz, DMSO) δ 0.86 (3H, t, 7.1, CH_3), 1.42 (9H, s, $C(CH_3)_3$), 2.40 (2H, t, 6.2, CH_2), 2.85 (2H, t, 5.4, CH_2), 3.48–3.52 (10H, m, 5×CH_2), 3.56 (2H, t, 6.2, CH_2), 3.81–3.91 (2H, m, CH_2), 4.32 (2H, s, CH_2), 6.20 (1H, s, CH), 6.30 (2H, s, NH_2), 6.36 (1H, d, 9.7, CH), 6.42 (1H, s, CH), 6.76–6.82 (2H, m, 2×CH),6.89–6.93 (3H, m, 3×CH), 7.88 (1H, d, 8.7, CH). ^{13}C NMR (100.62 MHz, DMSO) δ 13.63, 27.76, 35.81, 66.22, 69.65. HRMS 693.3018 [$(M+H)^+$] ($C_{37}H_{44}O_{11}N_2$ requires 693.3020).

*4.2.5. tert-Butyl 1-{9-[5-(1,2-dithiolan-3-yl)pentanamido]-2-[(ethoxycarbonyl)phenyl]-3-oxo-3H-xanthen-6-yloxy}-2-oxo-6,9,12-trioxa-3-azapentadecan-15-oate (**5**).* Thioctic acid (0.107 g, 0.210 mmol) and DIC (0.132 g, 0.520 mmol) were added to the solution of **4** (0.142 g, 0.210 mmol) in DCM. After stirring for 48 h at room temperature the reaction mixture was concentrated under reduced pressure. The residue was subjected to silica gel chromatography eluting with MeOH/DCM (0.1:9.9), then (0.5:9.5) giving 0.18 g of title compound as a yellow solid (97%). ^{1}H NMR (400 MHz, acetone) δ 0.95 (3H, t, 7.2, CH_3), 1.49 (9H, s, $C(CH_3)_3$), 1.69–1.75 (6H, m, 3×CH_2), 1.90–1.95 (2H, m, CH_2), 2.35 (2H, t, 6.5, CH_2), 2.45 (2H, t, 6.5, CH_2), 3.11–3.20 (2H, m, CH_2), 3.50–3.64 (12H, m, 6×CH_2), 3.55 (2H, t, 5.2, CH_2), 3.95–4.01 (2H, m, CH_2), 4.60 (2H, s, CH_2), 6.44 (1H, s, CH), 6.48 (1H, s, CH), 6.55 (1H, d, 9.7, CH), 6.79 (1H, d, 8.9, CH), 6.83 (1H, d, 8.6, CH), 6.97–7.07 (3H, m, 3×CH), 8.08 (1H, d, 8.6, CH). ^{13}C NMR (100.62 MHz, DMSO) δ 25.64, 26.28, 26.74, 28.34, 29.41,

29.44, 30.40, 30.43, 70.26. HRMS 881.3327 [(M+H)$^+$] ($C_{45}H_{57}O_{12}N_2S_2$ requires 881.3347).

*4.2.6. 1-(9-{5-[5-(1,2-Dithiolan-3-yl) pentanamido]-2-(ethoxycarbonyl)phenyl}-3-oxo-3H-xanthen-6-yloxy)-2-oxo-6,9,12-trioxa-3-azapentadecan-15-oic acid (6-aminofluorescein linker) (**6**).* TFA (3 ml, 99.5%) was added to the solution of **5** (0.18 g) in DCM (3 ml). After stirring for 3 h at room temperature DCM and TFA were removed under reduced pressure. The residue was solidified by addition of diethyl ether, then it was filtered and washed with the same solvent and dried to afford the title compound as a yellow solid (0.165 g, 98%). ^{1}H NMR (400 MHz, acetone) δ 0.92 (3H, t, 7.1, CH_3), 1.57–1.65 (6H, m, 3×CH_2), 2.18–2.20 (2H, m, CH_2), 2.49–2.55 (5H, m, 2×CH_2, CH), 3.53–3.92 (16H, m, 8×CH_2), 3.90–3.93 (2H, m, CH_2), 4.72 (2H, s, CH_2), 6.27 (1H, s, CH), 6.42 (1H, d, 9.7, CH), 6.62 (1H, s, CH), 6.92–6.98 (2H, m, 2×CH), 7.03–7.14 (3H, m, 3×CH), 8.00 (1H, d, 8.7, CH). ^{13}C NMR (100.62 MHz, $CDCl_3$) δ 23.04, 24.62, 39.70, 43.66. HRMS 639.20+188.00 (TA) [(M+H)$^+$] ($C_{41}H_{50}O_{12}S_2N_2$ requires 826.20).

4.3. Synthesis of the fluorescein linker

*4.3.1. tert-Butyl 10-{[(9H-fluoren-9-yl) methoxy]carbonylamino}-2,2-dimethyl-4,11-dioxo-3,5,18,21-tetraoxa-5,12-diazatetracosan-24-oate (**10**).* tert-Butyl-12-amino-4,7,10-trioxadodecanoate (0.148 g, 0.53 mmol) and DIC (0.074 g, 0.58 mmol) were added to the solution of 2-(*N*-Fmoc), 6-(*N*-Boc)-diamino caproic acid (0.250 g, 0.53 mmol) in DCM. After stirring for 24 h at room temperature the reaction mixture was filtered and concentrated under reduced pressure. The residue was subjected to silica gel chromatography eluting with pet. ether/EtOAc (2.5:7.5) to afford the title compound as a white solid (0.358 g, 92%). ^{1}H NMR (400 MHz, $CDCl_3$) δ 1.25–1.28 (2H, m, CH_2), 1.30–1.41 (2H, m, CH_2), 1.44 (18H, s, 2×$C(CH_3)_3$), 1.48–1.53 (2H, m, CH_2), 2.47 (2H, t, 6.5, CH_2), 3.11 (2H, s, CH_2), 3.47 (2H, s, CH_2), 3.55–3.60 (10H, m, 5×CH_2), 3.68 (2H, t, 8.8, CH_2), 4.10–4.17 (1H, m, CH), 4.20–4.24 (1H, m, CH), 4.40–4.42 (2H, m, CH_2), 7.30 (2H, t, 7.4, 2×CH), 7.39 (2H, t, 7.4, 2×CH), 7.60 (2H, d, 7.4, 2×CH), 7.76 (2H, d, 7.4, 2×CH). ^{13}C NMR (100.62 MHz, $CDCl_3$) δ 22.73, 28.34, 28.69, 29.89, 36.43, 39.58, 47.43, 67.10, 69.86, 70.56, 70.66, 70.77, 120.22, 125.33, 127.33, 127.96, 141.55. HRMS 506.30+223.00 (Fmoc) [(M+H)$^+$] ($C_{39}H_{58}O_{10}N_3$ requires 728.88).

*4.3.2. tert-Butyl 5-(4-aminobutyl)-1-(9H-fluoren-9-yl)-3,6-dioxo-2,10,13,16-tetraoxa-4,7-diazanonadecan-19-oate (**11**).* $BiCl_3$ (0.030 g, 0.096 mmol) was added to a solution of **10** (0.350 g, 0.48 mmol) in acetonitrile/water (5 ml/100 μl). The reaction mixture was stirred at 55 °C for 5 h. Additional portions of $BiCl_3$ (0.030 g, 0.096 mmol) were added after 1 and 3 h from reaction start. Then solid $NaHCO_3$ was added and the reaction mixture was filtered and concentrated under reduced pressure. The residue was subjected to silica gel chromatography eluting with MeOH/DCM (1:9), then (2:8) giving 0.094 g of the title compound (31%) as a colourless solid. ^{1}H NMR (400 MHz, $CDCl_3$) δ 1.40(9H, s, $C(CH_3)_3$), 1.51–1.58 (2H, m, CH_2), 1.81–1.91 (4H, m, 2×CH_2), 2.46 (2H, t, 6.3, CH_2), 3.03–3.05 (2H, m, CH_2), 3.57–3.69 (14H, m, 7×CH_2), 4.17 (1H, t, 7.0, CH), 7.27 (2H, t, 8.6, 2×CH), 7.35 (2H, t, 7.3, 2×CH), 7.59 (2H, d, 7.3, 2×CH), 7.72 (2H, d, 7.5, 2×CH). ^{13}C NMR (100.62 MHz, $CDCl_3$) δ 28.34, 39.33, 47.32, 67.14, 120.13, 125.50, 127.36, 127.91, 141.46. HRMS 628.3596 [(M+H)$^+$] ($C_{34}H_{49}O_8N_3$ requires 628. 3592).

*4.3.3. tert-Butyl 5-{4-[5-(1,2-dithiolan-3-yl) pentanamido]butyl}-1-(9H-fluoren-9-yl)-3,6-dioxo-2,10,13,16-tetraoxa-4,7-diazanonadecan-19-oate (**12**).* Thioctic acid (0.036 g, 0.176 mmol) and DIC (0.022 g, 0.176 mmol) were added to the solution of **11** (0.092 g, 0.146 mmol) in DCM with a few drops of Et_3N. After stirring for 24 h at room temperature the reaction mixture was concentrated under reduced pressure. The residue was subjected to silica gel chromatography eluting with EtOAc, then MeOH/DCM (1:9) giving 0.035 g of the title compound (29%) as a slightly yellow solid. ^{1}H NMR (400 MHz, $CDCl_3$) δ 1.41 (9H, s, $C(CH_3)_3$), 1.48–1.56 (2H, m, CH_2), 1.62–1.74 (10H, m, 5×CH_2), 1.87–1.95 (2H, m, CH_2), 2.15 (2H, t, 4.4, CH_2), 2.42–2.44 (1H, m, CH), 2.45 (2H, t, 6.4, CH_2), 3.08–3.21 (4H, m, 2×CH_2), 3.46–3.60 (12H, m, 6×CH_2), 3.67 (2H, t, 6.5, CH_2), 4.20–4.22 (1H, m, CH), 7.30 (2H, t, 7.7, 2×CH), 7.39 (2H, t, 7.7, 2×CH), 7.61 (2H, d, 4.5, 2×CH), 7.76 (2H, d, 7.5, 2×CH). ^{13}C NMR (100.62 MHz, $CDCl_3$) δ 22.69, 22.81, 23.57, 24.68, 24.72, 25.63, 28.30, 28.64, 28.90, 28.94, 29.11, 33.87, 33.91, 34.80, 34.84, 36.41, 36.62, 38.65, 38.69, 39.11, 39.59, 40.42, 42.61, 47.39, 56.51, 56.62, 67.06, 67.21, 69.76, 70.43, 70.51, 70.61, 70.72, 120.20, 125.32, 127.30, 127.95, 141.50, 144.00, 172.20, 173.32, 178.23. HRMS 833.4197 [(M+NH_4)$^+$] ($C_{42}H_{61}O_9N_3S_2$ requires 833.4187).

*4.3.4. tert-Butyl 15-amino-25-(1,2-dithiolan-3-yl)-14,21-dioxo-4,7,10-trioxa-13,20-diazapentacosan-1-oate (**13**).* Compound **12** (0.033 g, 0.040 mmol) was stirred for 2 h at room temperature with 20% piperidine in CH_3CN. Then the reaction mixture was concentrated under reduced pressure. The residue was dissolved in EtOH and concentrated again giving 0.022 g of the title compound (92%) as a slightly yellow solid. HRMS 594.3244 [(M+H)$^+$] ($C_{27}H_{51}O_7N_3S_2$ requires 594.3241).

*4.3.5. tert-Butyl 25-(1,2-dithiolan-3-yl)-15-({2-[9-(2-ethoxycarbonyl)phenyl]-3-oxo-3H-xanthen-6-yloxy}acetamido)-14,21-dioxo-4,7,10-trioxa-13,20-diazapentacosan-1-oate (**14**).* Compound **9** (0.015 g, 0.036 mmol) was dissolved in small amount of DMF. HATU (0.017 g, 0.044 mmol) and DIPEA (0.014 g, 0.11 mmol) were added. After stirring for 15 min at room temperature, **14** (0.022 g, 0.036 mmol) was added. The reaction mixture was stirred for 3 h at room temperature, then another portion of HATU (0.017 g, 0.044 mmol) and DIPEA (0.014 g, 0.11 mmol) were added. After stirring for 20 h at room temperature the reaction mixture was diluted with water (50 ml), extracted with Et_2O (3×20 ml). The organic phase was dried over anhydrous Na_2SO_4, then filtered and concentrated under reduced pressure. The residue was subjected to silica gel chromatography eluting with MeOH/DCM (0.5:9.5) giving 0.022 g of the title compound (60%) as a yellow solid. ^{1}H NMR (400 MHz, $CDCl_3$) δ 0.84 (3H, t, 10.6, CH_3), 1.44 (9H, s, $C(CH_3)_3$), 1.51–1.59 (2H, m, CH_2), 1.62–1.73 (10H, m, 5×CH_2), 1.90–1.95 (2H, m, CH_2), 2.10–2.20 (2H, m, CH_2), 2.35–2.40 (2H, m, CH_2), 2.45–2.54 (1H, m, CH), 3.09–3.20 (4H, m, 2×CH_2), 3.38–3.41 (2H, m, CH_2), 3.47–3.59 (10H, m, 5×CH_2), 3.60–3.64 (2H, m, CH_2), 4.03–4.05 (2H, m, CH_2), 4.20–4.22 (1H, m, CH), 4.81 (2H, s, CH_2), 6.47 (1H, s, CH), 6.55 (1H, d, 10.4, CH), 6.82–7.01 (4H, m, 4×CH), 7.66–7.77 (3H, m, 3×CH), 8.27 (1H, d, 10.6, CH). ^{13}C NMR (100.62 MHz, $CDCl_3$) δ 14.24, 23.65, 23.96, 24.77, 25.35, 25.79, 26.77, 29.13, 29.36, 30.57, 33.32, 34.99, 38.70, 38.95, 40.45, 42.51, 42.88, 46.90, 56.53, 56.69, 68.37, 107.94, 113.63, 119.93, 121.20, 127.25, 128.93, 131.07. HRMS 994.4192 [(M+H)$^+$] ($C_{51}H_{67}O_{13}N_3S_2$ requires 994.4188).

*4.3.6. 25-(1,2-Dithiolan-3-yl)-15-(2-{9-[2-(ethoxycarbonyl)phenyl]-3-oxo-3H-xanthen-6-yloxy}acetamido)-14,21-dioxo-4,7,10-trioxa-13,20-diazapentacosan-1-oic acid (fluorescein linker) (**15**).* Compound **14** (0.022 g, 0.022 mmol) was stirred with TFA (2 ml) and DCM (2 ml) at room temperature for 3 h. Then the reaction mixture was concentrated under reduced pressure, and dried on high vacuum line for 48 h. Title compound (0.012 g) was formed (57%) as a yellow solid. ^{1}H NMR (400 MHz, $CDCl_3$) δ 0.88–0.972 (3H, m, CH_3), 1.514–1.701 (14H, m, 7×CH_2), 2.33–2.38 (2H, m, CH_2), 2.42–2.53 (1H, m, CH), 3.11–3.18 (4H, m, 2×CH_2), 3.40–3.50 (2H, m, CH_2), 3.59–3.66 (12H, m, 6×CH_2), 4.03–4.06 (2H, m, CH_2), 4.21–4.24 (1H, m, CH), 4.81 (2H, s, CH_2), 6.46 (1H, s, CH), 6.55 (1H, d, 9.6, CH), 6.82–7.00 (4H, m, 4×CH), 7.67–7.73

(3H, m, 3×CH), 8.25 (2H, d, 8.0, CH). ^{13}C NMR (100.62 MHz, $CDCl_3$) δ 11.16, 14.24, 23.18, 23.67, 23.97, 24.74, 25.78, 29.14, 30.58, 32.94, 38.96, 42.50, 68.38, 129.01, 131.08. HRMS 936.3420 [$(M-H)^-$] ($C_{47}H_{59}O_{13}N_3S_2$ requires 936.3417), 938.3560 [$(M+H)^+$] ($C_{47}H_{59}O_{13}N_3S_2$ requires 938.3562).

4.4. Synthesis of the TAMRA linker

*4.4.1. tert-Butyl-10-amino-2,2-dimethyl-4,11-dioxo-3,15,18,21-tetraoxa-5,12-diazatetracosan-24-oate (**16**).* Compound **10** (0.055 g, 0.068 mmol) was stirred with 20% piperidine in CH_3CN for 2 h at room temperature. Then the reaction mixture was concentrated under reduced pressure. The residue was dissolved in EtOH and concentrated again giving 0.035 g of the title compound (92%) as a white solid. HRMS 506.3430 [$(M+H^+)$] ($C_{24}H_{47}O_8N_3$ requires 506.3436).

*4.4.2. tert-Butyl-10-[5-(1,2-dithiolan-3-yl) pentanamido]-2,2-dimethyl-4,11-dioxo-3,5,18,21-tetraoxa-5,12-diazatetracosan-24-oate (**17**).* Thioctic acid (0.021 g, 0.103 mmol) and DIC (0.013 g, 0.103 mmol) were added to the solution of **16** (0.035 g, 0.069 mmol) in DCM. After stirring for 24 h at room temperature the reaction mixture was filtered and concentrated under reduced pressure. The residue was subjected to silica chromatography eluting with EtOAc, then MeOH/DCM (1:9) giving 0.040 g of the title compound (85%) as a slightly yellow oil. ^{1}H NMR (400 MHz, $CDCl_3$) δ 1.33–1.45 (2H, m), 1.47 (18H, s, 2×$C(CH_3)_3$), 1.64–1.95 (10H, m), 2.21 (2H, t, 7.5, CH_2), 2.36 (2H, t, 7.4, CH_2), 2.44–2.48 (1H, m, CH), 2.50 (2H, t, 6.5, CH_2), 3.45–3.65 (12H, m), 3.71 (2H, t, 6.5, CH_2), 4.40 (1H, q, 7.1, CH). ^{13}C NMR (100.62 MHz, $CDCl_3$) δ 14.51, 22.84, 25.61. 28.43, 28.77, 29.17, 34.94, 36.59, 38.78, 39.65, 40.54, 53.12, 67.23, 69.92, 70.62, 70.69, 70.81, 70.91. HRMS 711.4030 [$(M+NH_4)^+$] ($C_{32}H_{59}O_9N_3S_2$ requires 711.4031).

*4.4.3. 15-(4-Aminobutyl)-21-(1,2-dithiolan-3-yl)-14,17-dioxo-4,7,10-trioxa-13,16-diazahenicosan-1-oic acid (**18**).* TFA (3 ml) was added to the solution of **17** (0.040 g, 0.057 mmol) in DCM (3 ml). After stirring for 3 h at room temperature DCM and TFA were removed under reduced pressure. The residue was solidified by addition of diethyl ether, then it was filtered, washed with the same solvent and dried to afford the title compound as a yellow oil (0.027 g, 89%). ^{1}H NMR (400 MHz, $CDCl_3$) δ 1.33–1.45 (2H, m), 1.64–1.95 (10H, m), 2.21 (2H, t, 7.5, CH_2), 2.36 (2H, t, 7.4, CH_2), 2.44–2.47 (1H, m, CH), 2.48 (2H, t, 6.5, CH_2), 3.55–3.80 (14H, m, 7×CH_2), 4.47 (1H, q, 7.1, CH). ^{13}C NMR (100.62 MHz, $CDCl_3$) δ 23.30, 43.20, 70.44, 120.71. HRMS 538.50 [$(M+H)^+$] ($C_{23}H_{44}O_7N_3S_2$ requires 538.62).

*4.4.4. 5-{14-[5-(1,2-Dithiolan-3-yl)pentanamido]-1-carboxy-13-oxo-3,6,9-trioxa-12-azaoctadecan-18-ylcarbamoyl}-2-[6-(dimethylamino)-3H-xanthen-9-yl]benzoate (TAMRA linker) (**19**).* 5-Carboxytetramethylrhodamine-*N*-succinimidyl ester (TAMRA SE) (0.005 g, 0.0095 mmol) was dissolved in CH_3CN. Compound **18** (0.0066 g, 0.0123 mmol) and resin—morpholinomethyl polystyrene (0.012 g, 1×10^{-3} mol/g) were added. After stirring for 24 h at room temperature the reaction mixture was filtered and concentrated under reduced pressure. The residue was subjected to silica gel chromatography eluting with MeOH/DCM (1:9), then (2:9) giving 0.0033 g of the title compound (37%) as a pink solid. HRMS 950.4041 [$(M+H)^+$] ($C_{48}H_{64}O_{11}N_5S_2$ requires 950.4038).

4.5. Preparation of colloids and functionalized nanoparticles

4.5.1. 18 (1) and 50 (2) nm gold colloid. Sodium tetrachloroaurate (1) (0.05 g, 0.14 mmol); (2) (0.0575 g, 0.161 mmol) was dissolved in 10 ml of water, then added to 500 ml of water and brought to boil. Sodium tricitrate (1) (0.075 g, 0.25 mmol) (2) (0.0605 g, 0.20 mmol) was dissolved in 10 ml of water, then added to the reaction mixture. The reaction mixture was left at boiling temperature for 15 min then cooled down to room temperature. To calculate the colloid concentration Beer–Lambert equation was used with gold extinction coefficient value 2.4×10^8[21] for 18 nm Au and 1.469×10^{10} for 46 nm Au nanoparticles.[38]

4.5.2. 40 nm silver citrate stabilized colloid. Water (500 ml) was heated to 45 °C, then silver nitrate (0.09 g, 0.53 mmol) dissolved in 10 ml of water was added. The reaction mixture was heated to 98 °C, then sodium citrate (0.11 g, 0.37 mmol) dissolved in 10 ml of water was added. The reaction mixture was kept for 90 min at 98 °C, then cooled down to room temperature. The concentration of colloid was calculated from Beer–Lambert equation using silver extinction coefficient value 2×10^{10}.[39]

4.5.3. 40 nm Silver EDTA stabilized colloid. Ethylenediaminetetraacetic acid (EDTA) (0.095 g, 0.32 mmol) was dissolved in 2000 ml of water. Sodium hydroxide (0.35 g, 8.75 mmol) was dissolved in 20 ml of water, then added to the reaction mixture. The reaction mixture was brought to boil then silver nitrate (0.088 g, 0.52 mmol) dissolved in 20 ml of water was added. The reaction mixture was kept at boiling temperature for 15 min, then it was cooled down to room temperature. The concentration of colloid was calculated from Beer–Lambert equation using silver extinction coefficient value 2×10^{10}.[39]

4.6. Synthesis of 4-(4,6-dimethoxy-1,3,5-triazin-2-yl)-4-methylmorpholinium chloride—DMT MM

DMT MM was synthesized as previously described by Kunishima et al.[35,36] 2-Chloro-4,6-dimethoxy-1,3,5-triazine (CDMT) (0.386 g, 2.2 mmol) was dissolved in THF. Then *N*-methylmorpholine (NMM) (0.202 g, 2.0 mmol) dissolved in THF was added. The reaction mixture was stirred for 30 min at room temperature. Formed white solid was filtered off, washed with THF, dried to give DMT MM (0.46 g, 75%). ^{1}H NMR (400 MHz, D_2O) δ 3.61 (3H, s, CH_3), 3.88–4.01 (4H, m, 2×CH_2), 4.14–4.20 (2H, m, CH_2), 4.23 (6H, s, 2×CH_3), 4.68–4.74 (2H, m, CH_2). ^{13}C NMR (100.62 MHz, D_2O) δ 55.25, 56.59, 59.55, 61.55, 173.38. HRMS 241.1295 [$(M+H)^+$] ($C_{10}H_{17}O_3N_4$ requires 241.1295).

4.7. Nanoparticles (Au (18, 46 nm), Ag citrate, Ag EDTA)–linkers conjugates preparation

The concentration of the colloid was calculated from Lambert–Beer equation. The amount of the linker solution in MeOH (1×10^{-3} M), which has to be added was calculated based on found earlier number of linker molecules, which attached to one nanoparticle (Table 1) (2 equiv excess of the linker solution was used in each case). The linker solution was added to the nanoparticles solution, then left over night at room temperature. The nanoparticles were then spun down (20 min, 7000 rpm), supernatants were discarded, the pellets washed with H_2O, then centrifuged again (20 min, 7000 rpm). The supernatants were discarded, the pellets resuspended in the desired volume of water or buffer.

4.8. Nanoparticle–linker–DNA conjugates preparation

Nanoparticle–linker conjugates were prepared as described above, then they were resuspended in 1×PBS buffer (10 mM, pH=7.6). *N*-(3-Dimethylaminopropyl)-*N*′-ethyl carbodiimide hydrochloride (EDC·HCl, 1.04×10^{-5} mol/ml, 2 equiv) and *N*-hydroxysulfosuccinimide (sulfo NHS, 9.21×10^{-6} mol/ml, 2 equiv) were added. The sample was shaken for 30 min, then DNA was added (100 pmol/μl, 2 equiv). Sample was shaken overnight, then spun

down for 20 min at 7000 rpm. The supernatant was discarded, the pellet resuspended in the desired volume of 0.3 M or 0.1 M NaCl in 10 mM PBS buffer (pH=7.2). If the DMT MM was used prepared nanoparticle–linker conjugates were resuspended in 1×PBS buffer (10 mM, pH=7.6) or H_2O. Then DMT MM (7.22×10^{-6} mol/ml, 2 equiv) and DNA (100 pmol/μl, 2 equiv) were added at the same time. Sample was shaken overnight, then spun down (20 min, 6500 rpm). The supernatant were discarded, the pellet resuspended in the desired amount of 0.3 M or 0.1 M NaCl in 10 mM PBS buffer (pH=7.2). The concentration of the probe was found from Beer–Lambert equation.

4.9. Zeta particle size and zeta potential measurements

Malvern High Performance Particle Sizer was used to measure the zeta size of formed conjugates. Linker functionalized nanoparticles were prepared as described above. Nanoparticle–linker–DNA conjugates were prepared in water, in the presence of DMT MM, using the protocol described above. All prepared conjugates were washed with water (500 μl), then centrifuged for 20 min at 6500 rpm. The supernatants were discarded, pellets resuspended in water (500 μl). UV–vis spectra of all samples were taken in order to calculate probes concentrations. The samples were prepared by dilution of prepared solutions with water to the following concentrations: for 18 nm Au conjugates 7.95×10^{-10} M; for 50 nm Au conjugates 2.52×10^{-11} M, for both types of silver nanoparticles 3×10^{-11} M; 1 ml of each sample was used.

Samples for zeta potential measurements were prepared in the same way as samples for DLS, but they were diluted to the following concentrations: 2.65×10^{-10} M for 18 nm Au conjugates, 8.4×10^{-12} M for 50 nm Au conjugates, 1×10^{-11} M for silver nanoparticles conjugates; 3 ml of each sample was used. Malvern Zetasizer 2000 was used to measure the zeta potential of all probes.

4.10. Gel electrophoresis

Agarose gels of 1.5% were prepared by heating 1.5 g of agarose in 100 ml of 0.5×TBE buffer. Linker–nanoparticle and DNA–linker–nanoparticle conjugates were prepared as described above, the concentration of prepared samples was calculated using the Beer–Lambert equation. The concentration of the samples loaded on the gel was kept constant: for 18 nm Au nanoparticles conjugates: 3.63×10^{-8} M, for 50 nm Au nanoparticles conjugates: 1.14×10^{-9} M, for Ag citrate nanoparticles conjugates: 1.16×10^{-9} M, for Ag EDTA nanoparticles conjugates: 6.86×10^{-10} M. The calculated volumes of each sample was diluted to 10 μl, then 10 μl of 10% glycerol was added before loading the samples in the gel wells. The gels were run for 60 min at 120 mV.

4.11. SERS analysis

All SERS spectra were recorded using a Leica DM/LM microscope equipped with an Olympus 20×/0.4 long working distance objective, which was used to collect 180° backscattered light from a microtiter plate. The spectrometer system was Renishaw inVia with 632.8 nm line of helium–neon laser or 514 nm Ar ion laser or 785 nm Diode laser coupled to a Renishaw Ramascope System 2000.

References and notes

1. Thaxton, S. D.; Georganopoulou, G. D.; Mirkin, C. A. *Clin. Chim. Acta* **2006**, *363*, 120.
2. Storhoff, J. J.; Elghanian, R.; Mucic, R. C.; Mirkin, C. A.; Letsinger, R. L. *J. Am. Chem. Soc.* **1998**, *120*, 1959.
3. Cao, Y. C.; Jin, R.; Thaxton, C. S.; Mirkin, C. A. *Talanta* **2005**, *67*, 449.
4. Thompson, D. G.; Stokes, R. J.; Martin, R. W.; Lundahl, P. J.; Faulds, K.; Graham, D. *Small* **2006**, *4*, 1054.
5. Dougan, J. A.; Karlsson, C.; Smith, W. E.; Graham, D. *Nucleic Acids Res.* **2007**, *35*, 3668.
6. Graham, D.; Faulds, K.; Smith, W. E. *Chem. Commun.* **2006**, 4363.
7. Graham, D.; Faulds, K.; Smith, W. E. *Analyst* **2005**, *130*, 1125.
8. Graham, D.; Smith, W. E.; Linacre, A. M.; Munro, C. H.; Watson, N. D.; White, P. C. *Anal. Chem.* **1997**, *69*, 4703.
9. Graham, D.; Thompson, D. G.; Smith, W. E.; Faulds, K. *Nat. Nanotechnol.* **2008**, *3*, 548.
10. Faulds, K.; Stewart, L.; Smith, W. E.; Graham, D. *Talanta* **2005**, *67*, 667.
11. Faulds, K.; Barbagello, K. P.; Kerr, J. T.; Smith, W. E.; Graham, D. *Analyst* **2004**, *76*, 412.
12. Faulds, K.; Smith, W. E.; Graham, D. *Anal. Chem.* **2004**, *76*, 412.
13. Adamczyk, M.; Grote, J. *Bioorg. Med. Chem. Lett.* **2000**, *10*, 1539.
14. Sameiro, M.; Goncalves, T. *Chem. Rev.* **2009**, *109*, 190.
15. Klonis, N.; Sawyer, W. H. *Photochem. Photobiol.* **2000**, *72*, 179.
16. Gao, J.; Wang, P.; Giese, R. W. *Anal. Chem.* **2002**, *74*, 6397.
17. Orndorff, W. R.; Hemmer, A. J. *Fluorescein and Some of its Derivatives* Contribution from the Baker Laboratory of Chemistry; Cornell University: Ithaca, New York, NY, 1927.
18. Hurd, C. D.; Schmerlin, L. *Alkenyl Derivatives of Fluorescein* Contribution from the Chemical Laboratory of Northwestern University; Evanston, Illinois, 1937.
19. Falck, J. R.; Krieger, M.; Goldstein, J. L.; Brown, M. S. *J. Am. Chem. Soc.* **1981**, *103*, 7396.
20. Burchak, O. N.; Mugherli, L.; Chatelain, F.; Balakirev, M. Y. *Bioorg. Med. Chem.* **2006**, *14*, 2559.
21. Lohse, J.; Nielsen, P. E.; Harhit, N.; Dahl, O. *Bioconjugate Chem.* **1997**, *8*, 503.
22. Elghanian, R.; Storhoff, J. J.; Mucic, R. C.; Letsinger, R. L.; Mirkin, C. A. *Science* **1997**, *277*, 1078.
23. Demers, L. M.; Mirkin, C. A.; Mucic, R. C.; Reynolds, R. A.; Letsinger, R. L.; Elghanian, R.; Viswanadham., G. *Anal. Chem.* **2000**, *72* (22), 5535.
24. Lee, J. S.; Lytton-Jean, A. K. R.; Hurst, S. J.; Mirkin, C. A. *Nano Lett.* **2007**, *7*, 2112.
25. Li, Z.; Jin, R.; Mirkin, C. A.; Letsinger, R. L. *Nucleic Acids Res.* **2002**, *30*, 1558.
26. He, M.; Musick, M. D.; Nicewarner, S. R.; Salinas, F. G.; Benkovic, S. J.; Natan, M. J.; Keating, C. D. *J. Am. Chem. Soc.* **2000**, *122*, 9071.
27. Elghanian, R.; Storhoff, J. J.; Mucic, R. C.; Letsinger, R. L.; Mirkin, C. A. *Science* **1997**, *277*, 1078.
28. Thompson, D. G.; Enright, A.; Faulds, K.; Smith, W. E.; Graham, D. *Anal. Chem.* **2008**, *80*, 2805.
29. Vidal, B. C., Jr.; Deivaraj, T. C.; Yang, J.; Too, H. P.; Chow, G. M.; Gan, L. M.; Lee, J. Y. *New J. Chem.* **2005**, *29*, 812.
30. McKenzie, F.; Ingram, A.; Stokes, R.; Graham, D. *Analyst* **2009**, *134*, 549.
31. Nguyen, T.; Francis, M. B. *Org. Lett.* **2003**, *5*, 3245.
32. Kazzouli, S. E.; Koubachi, J.; Berteina-Raboin, S.; Mouaddib, A.; Guillaumet, G. *Tetrahedron Lett.* **2006**, *47*, 8575.
33. Navath, R. S.; Pabbisetty, K. B.; Hu, L. *Tetrahedron Lett.* **2006**, *47*, 389.
34. Zanchet, D.; Micheel, C. M.; Parak, W. J.; Gerion, D.; Alivisatos, A. P. *Nano Lett.* **2001**, *1*, 32.
35. Kunishima, M.; Kawachi, C.; Morita, J.; Terao, K.; Iwasaki, F.; Tani, S. *Tetrahedron* **1999**, *55*, 13159.
36. Kunishima, M.; Kawachi, C.; Hioki, K.; Terao, K.; Tani, S. *Tetrahedron* **2001**, *57*, 1551.
37. McKenzie, F.; Stevens, V.; Ingram, A.; Graham, D. *Chem. Commun.* **2009**, 2872.
38. Courtesy of BBInternational Life Sciences.
39. Yugerabide, J.; Yguerabide, E. E. *Anal. Biochem.* **1998**, *262*, 157.